Dynamics simulations of excited-state triple proton transfer in 7-azaindole complexes with water, water–methanol and methanol

ARTICLE *in* JOURNAL OF PHOTOCHEMISTRY AND PHOTOBIOLOGY A: CHEMISTRY · AUGUST 2013

Impact Factor: 2.5 · DOI: 10.1016/j.jphotochem.2013.05.012

Journal of Photochemistry and Photobiology A: Chemistry 266 (2013) 28–36

Contents lists available at SciVerse ScienceDirect

Journal of Photochemistry and Photobiology A: Chemistry

journal homepage: www.elsevier.com/locate/jphotochem

Dynamics simulations of excited-state triple proton transfer in 7-azaindole complexes with water, water–methanol and methanol

Rathawat Daengngern[a], Khanittha Kerdpol[a], Nawee Kungwan[a,*], Supa Hannongbua[b], Mario Barbatti[c]

[a] Department of Chemistry, Faculty of Science, Chiang Mai University, Chiang Mai 50200, Thailand
[b] Department of Chemistry, Faculty of Science, Kasetsart University, Bangkhen Campus, Bangkok 10930, Thailand
[c] Max-Planck-Institut für Kohlenforschung, Kaiser-Wilhelm-Platz 1, D-45470 Mülheim an der Ruhr, Germany

ARTICLE INFO

Article history:
Received 14 February 2013
Received in revised form 26 March 2013
Accepted 24 May 2013
Available online 6 June 2013

Keywords:
Dynamics simulation
Excited-state proton transfer
Excited-state tautomerization
Water–methanol mixture
7-Azaindole
ADC(2)

ABSTRACT

Excited-state triple proton transfer (ESTPT) reactions in 7-azaindole (7AI) complexed with two water, with one water and one methanol, and with two methanol molecules were investigated by dynamics simulations in the first excited state computed with the second order algebraic-diagrammatic construction (ADC (2)) method. The results show that photoexcitation may trigger ultrafast an asynchronous concerted proton transfer via two solvent molecules along an intermolecular hydrogen-bonded network. The probability of occurrence of ESTPT ranges from 32% for 7AI(H_2O–MeOH) to 64% for 7AI(MeOH)$_2$. The average time for completing the ESTPT varies between 58 and 85 fs depending on the complex. The proton transfer (rather than hydrogen transfer) nature of the reaction was suggested by the nonexistence of crossings between the $\pi\pi^*$ and $\pi\sigma^*$ states.

1. Introduction

Excited-state proton transfer (ESPT) [1,2] is one important class of reactions in physical, chemical and biological phenomena, with uses in fluorescent probes [3–5], photostabilizers [6] and light-emitting devices [7,8]. Among many molecules undergoing ESPT, 7-azaindole (7AI) has been the most widely investigated by experimental and theoretical techniques [9–36]. All this attention paid to 7AI is owned to its potential as a model system for studying ESPT phenomena in several instances, such as DNA mutagenesis, proton relay in enzymes, and proton transport through membranes [37]. A more complete understanding of the multiple proton transfer processes occurring in 7AI complexed with solvent partners may shed the light on the occurrence of these important phenomena.

7AI is a bicyclic azaaromatic molecule comprising a pyrrole (proton donor) and a pyridine (proton acceptor) rings (Fig. 1). The proton donor and proton acceptor sites can form a hydrogen-bonded network upon dimerization in nonpolar solvents and in complexation with protic solvents such as ammonia, water and alcohol. The excited-state tautomerization of 7AI within water has been intensively studied in the condensed and gas phases with experimental and theoretical methods [21,23,30,38–41]. The excited-state multiple proton transfers in 7AI complexed with alcohol has been also thoroughly studied [15,21,22,29,32,42]. Most previous theoretical studies related to 7AI, however, were focused only on static calculations either in the ground state or excited state. Therefore, these studies could not provide a time-dependent picture of the proton transfer (PT) or hydrogen transfer (HT) reaction pathways. (The nature of the transfer, whether it is a PT or HT, depends on the energy of the $\pi\pi^*$ and $\pi\sigma^*$ states, as PTs occur along the $\pi\pi^*$ state whereas HTs occur along the $\pi\sigma^*$ state [43,44]. We will show that for the 7AI complexes investigated here, PT most likely takes place.)

To the best of our knowledge, there has been no theoretical investigation reported on the intermolecular ESPT dynamics in 7AI within mixed solvents such as water–methanol. 7-Hydroxyquinoine (7HQ) with mixed ammonia/water solvent-wire clusters was reported by Tanner et al. [44–46]. Their results showed that replacing NH_3 molecule with one or two water molecules stopped the hydrogen-atom transfer along the solvent wires. For 7AI with water, Kina et al. [40] performed dynamics simulations at the CASSCF level to study complexes with up two water molecules and simulations at the CASSCF/MM level to investigate water solvation effects. Their results showed that the complete ESIPT process was reached around 50 fs in 7AI(H_2O) and in the range of 40–60 fs

* Corresponding author. Tel.: +66 53 943341x101; fax: +66 53 892277.
E-mail addresses: naweekung@gmail.com, naweekung@hotmail.com (N. Kungwan).

1010-6030/$ – see front matter © 2013 Elsevier B.V. All rights reserved.
http://dx.doi.org/10.1016/j.jphotochem.2013.05.012

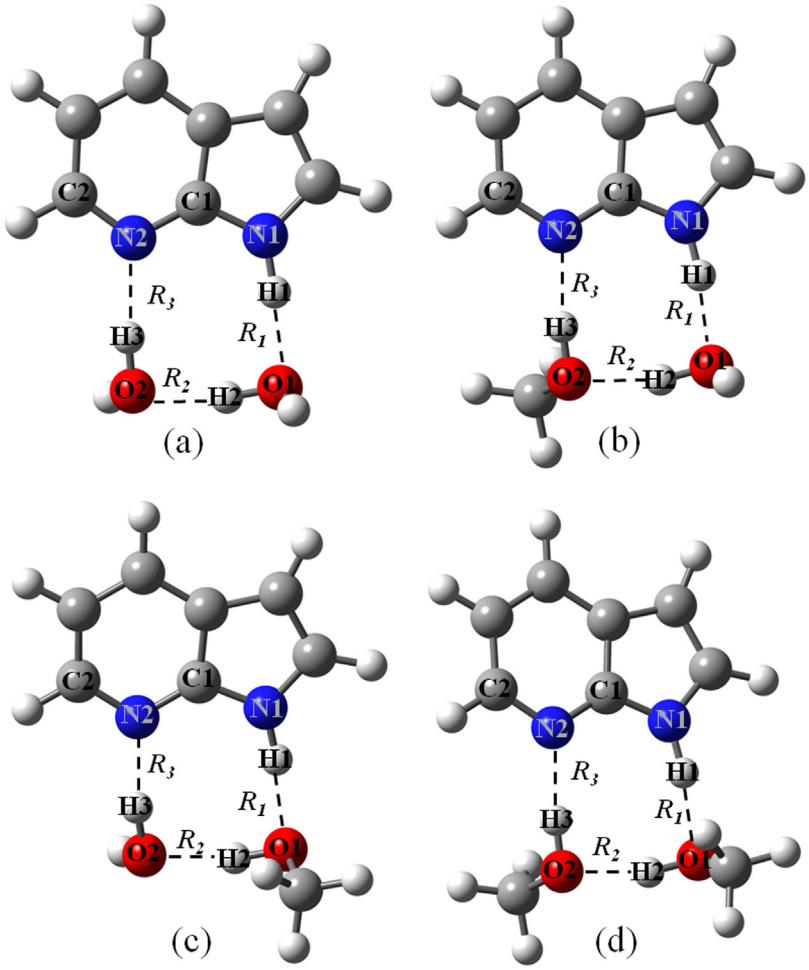

Fig. 1. Ground-state optimized structures of 7AI complexes at RI-ADC(2)/SVP-SV(P) level: (a) 7AI$(H_2O)_2$, (b) 7AI(H_2O–MeOH), (c) 7AI(MeOH–H_2O), and (d) 7AI$(MeOH)_2$. Intermolecular hydrogen bonds are indicated by dashed lines.

in 7AI$(H_2O)_2$ cluster. Another recent investigation using on-the-fly dynamics simulation was done by our group [20] on the excited-state multiple proton transfer reaction in the gas phase cluster of 7AI$(MeOH)_n$ (n = 1–3) using RI-ADC(2) level of theory. The results revealed that the PT in all clusters is complete within 84 fs, which was slower than that of 7AI$(H_2O)_{1,2}$ cluster. The difference in the ESPT time of 7AI$(H_2O)_n$ and 7AI$(MeOH)_n$ is reasonable because methanol is less polar than water.

Here, we simulated the PT dynamics of the 7AI$(H_2O)_2$, 7AI(MeOH–H_2O), and 7AI(H_2O–MeOH) complexes. Together with our previous data for 7AI$(MeOH)_2$ [20], we aim at systematically accessing the role of different solvents surrounding 7AI, the effect of mixing solvents, and the influence of different connections at the proton donor site (pyrrole moiety). Starting from a complex with two waters, the substitution of each water molecule by a methanol molecule should be very informative on PT dynamics in term of reaction probability and time constants.

2. Computational calculations

2.1. Static calculations

Ground-state optimizations of 7AI with water and mixed-solvent molecules, (a) 7AI$(H_2O)_2$, (b) 7AI(H_2O–MeOH), (c) 7AI(MeOH–H_2O) and (d) 7AI$(MeOH)_2$ complexes (Fig. 1) were calculated in the gas phase. The results for 7AI$(MeOH)_2$ have been reported before in Ref. [20]. These optimizations were done with the second-order algebraic diagrammatic construction method (ADC(2)) with the resolution-of-identity (RI) approximation for the electron-repulsion integrals [47,48], using the TURBOMOLE 5.10 program package [49,50]. The split valence polarized (SVP) basis set [51] was assigned to heavy atoms and hydrogen atoms involved in the hydrogen-bonded network, whereas the split valence (SV(P)) basis set was assigned to the remaining hydrogen atoms in the complexes. This level, hereafter referred as RI-ADC(2)/SVP-SV(P), is designed to keep the computational cost at an acceptable level, but still providing the accurate simulation results [20]. The minimum character of all optimized structures of 7AI with solvent clusters was confirmed by normal mode analysis. These optimized structures were further used for generating the initial conditions for excited-state dynamics simulations.

2.2. Excited-state dynamics simulation

Born–Oppenheimer dynamics simulations were carried out for 7AI$(H_2O)_2$, 7AI(H_2O–MeOH), 7AI(MeOH–H_2O) and 7AI$(MeOH)_2$ complexes in the first-excited state (S_1) at the RI-ADC(2)/SVP-SV(P) level. The results for 7AI$(MeOH)_2$ have been reported before in Ref. [20]. The initial conditions were generated using a harmonic-oscillator Wigner distribution for each normal mode. Dynamics and initial conditions were performed with the NEWTON-X program package [52,53] interfaced with TURBOMOLE. Twenty-five trajectories for each complex were simulated using a time step of 1 fs and maximum trajectory time of 300 fs. Statistical analysis was

Table 1
Summary of the ground-state structures computed at RI-ADC(2)/SVP-SV(P) level. Distances in Å, dihedral angles in degrees. $ø_1$ = N1C1N2C2, $ø_2$ = O1N1N2O2.

	Complex			
	7AI(H_2O)$_2$	7AI(H_2O–MeOH)	7AI(MeOH–H_2O)	7AI(MeOH)$_2$
R_1	1.739	1.738	1.731	1.730
R_2	1.716	1.714	1.698	1.698
R_3	1.822	1.796	1.817	1.789
N1—O1	2.775	2.773	2.766	2.765
O1—O2	2.680	2.680	2.662	2.662
O2—N2	2.803	2.771	2.798	2.767
$ø_1$	179.8	179.9	179.8	179.9
$ø_2$	−7.4	−9.8	−8.5	−11.8

Table 2
Summary of the excited-state dynamics performed at RI-ADC(2)/SVP-SV(P): number of trajectories following each of the three types of reactions (see text), ESPT probability, and average time to complete the first, second and third proton transfers (PT). Average distances at the PT time are given in parenthesis (in Å).

Complex	Reaction			ESPT probability	Time (fs)		
	ESPT ($\pi\pi^*$)	IC ($\pi\pi^*/S_0$)	No		PT1	PT2	PT3
7AI(H_2O)$_2$	9	2	14	0.36	50(1.299)	55(1.339)	58(1.270)
7AI(H_2O–MeOH)	8	6	11	0.32	46(1.328)	58(1.290)	60(1.311)
7AI(MeOH–H_2O)	11	1	13	0.44	71(1.279)	83(1.295)	85(1.332)
7AI(MeOH)$_2$	16	4	5	0.64	68(1.308)	81(1.271)	84(1.334)

carried out to provide information on average energies of each state, on internal coordinates, relative potential energy profiles and time evolution of the PT reactions along the hydrogen-bonded network. Average energy profiles were analyzed in terms of characteristic points along the reaction pathways, namely Normal (N), Intermediary Structure (IS), and Tautomer (T). N was chosen as the geometry at time zero. The IS1 point was assigned to the structure with the proton in the middle way between the pyrrole ring and the first solvent molecule. The IS2 point was assigned to the structure with a proton in the middle way between the two solvent molecules. The IS3 point was assigned to the structure with the proton in the middle way between the second solvent and the pyridine ring. The T point was selected right after last PT was completed. Furthermore, molecular orbitals of different electronic transitions were characterized for a representative trajectory of each complex.

3. Results and discussion

3.1. Ground-state structure

The ground-state structures of all complexes were optimized using RI-ADC(2)/SVP-SV(P) to study the effect of the surrounding homogeneous and inhomogeneous solvent. Intermolecular hydrogen bonds, other important bond distances and dihedral angles are summarized in Table 1 (see Fig. 1 for definitions).

The results show that there are three intermolecular hydrogen bonds in the cyclic network: first, R_1(O1···H1), the hydrogen bond between a proton donor on pyrrole ring and the nearest solvent molecule; second, R_2(O2···H2), between the solvent molecules; and third, R_3(N2···H3), between the second solvent molecule and the pyridine ring. The four complexes are not significantly different because of the structural similarity between water and methanol. Nevertheless, when a methanol molecule replaces a water molecule, the intermolecular hydrogen bonds become stronger, as evidenced by shorter hydrogen bonds. Even stronger hydrogen bonds are obtained with 7AI(MeOH)$_2$ complex, as shown in previous reports [20,29,31]. The optimized structure of 7AI is planar, as indicated by the dihedral angle $ø_1$ (N1C1N2C2) close to 180° for all complexes (Table 1). In addition, the hydrogen bonded network is also almost planar, as indicated by $ø_2$ (O1N1N2O2) absolute values smaller than 12°.

3.2. Excited-state dynamics simulations

The simulated trajectories for each complex were categorized into three types of reactions: (1) "ESPT" when a proton is completely transferred within simulation time; (2) "IC" when $S_1(\pi\pi^*)/S_0$ crossing is reached within simulation time; and (3) "No" (for "No Transfer") when a complete PT does not occur within the simulation time. The S_1/S_0 crossing in type 2 suggests that internal conversion should take place. This process will not, however, be investigated further in this work due to the limitations of the ADC(2), as a single-reference method, to deal with S_1/S_0 crossings. The number of trajectories following each type of reaction, the probability of PT, and average time of PT for each complex is summarized in Table 2. By definition, the transfer time from an atom X to an atom Y is taken as the time for which the X–H distance becomes equal to the H–Y distance [20]. This distance, averaged over all trajectories of type 1, is also given in Table 2.

To determine whether a hydrogen atom or a proton is transferred, the relative energy of the ground and excited states at the N, IS, and T points along hydrogen-bonded network for all complexes were computed for representative trajectories of type 1 (Figures S1–S4 of the Supplementary Data). For example, a potential energy diagram of the complete reaction for the 7AI(H_2O)$_2$ complex (Figure S1) shows that the $\pi\sigma^*$ lies over 70 kcal mol^{-1} above the $\pi\pi^*$ state for N, IS and T points. No crossing between these states was observed. This situation, which is the same for all trajectories, shows that dynamics takes place only on the $\pi\pi^*$ state, characterizing the transfer as a PT process.

3.2.1. 7AI(H_2O)$_2$ complex

From 25 trajectories of the 7AI(H_2O)$_2$ complex, 9 underwent excited-state triple proton transfer (ESTPT) reaction (type 1). Two trajectories achieved a region of degeneracy between $S_1(\pi\pi^*)$ and S_0 and could not be continued because of the limitation of the current method (type 2). The PT process did not take place in 14 trajectories during the simulation time (type 3). A back-PT reaction was also observed in some trajectories. Thus, the PT reaction probability is 36%.

Details of the PT process can be illustrated by analysis of a representative trajectory (Fig. 2). The atom numbering is the same as defined in Fig. 1(a). A normal (N) form is observed at time 0. The proton departs from the pyrrole ring to O1 atom of the nearest water

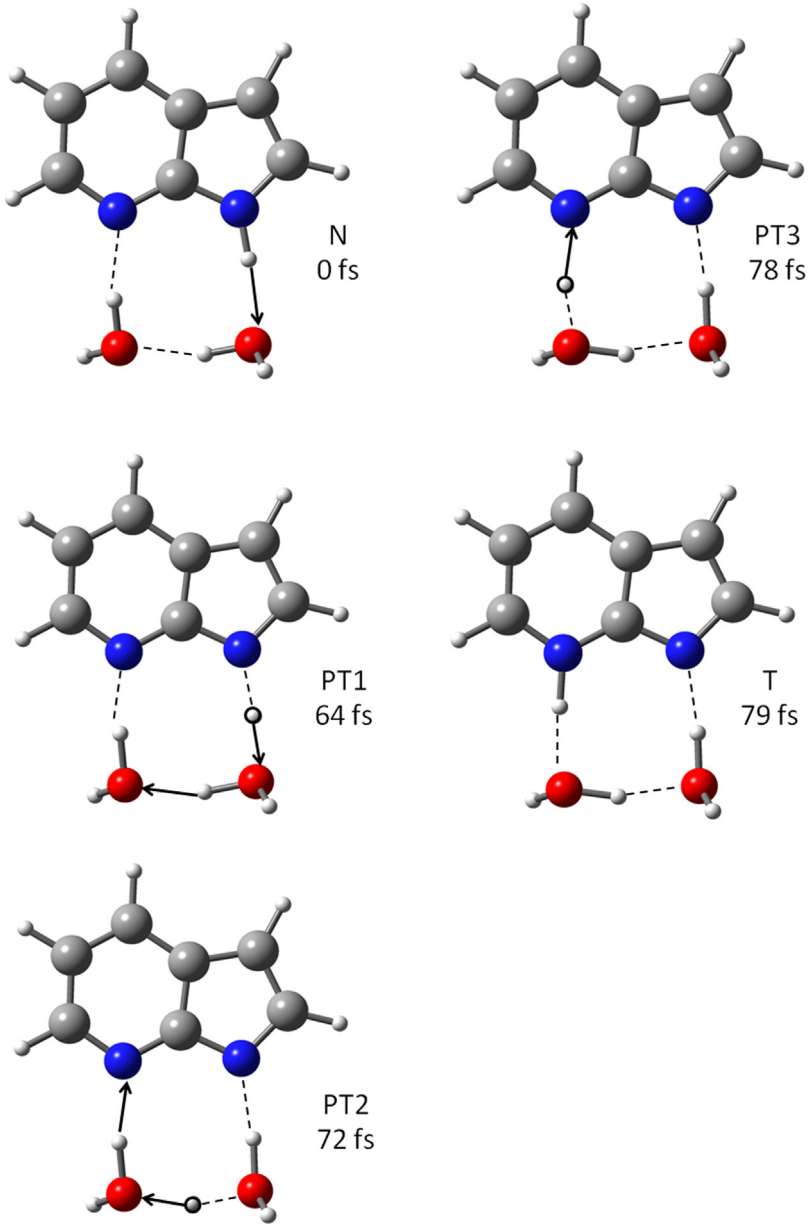

Fig. 2. Snapshots of a representative trajectory of the 7AI$(H_2O)_2$ complex showing the time evolution of the ESTPT reaction through a hydrogen-bonded network within 79 fs. Averaged over all type-1 trajectories, this reaction is completed within 58 fs. Normal (N), proton transfer (PT), and tautomer (T).

(PT1) at 64 fs, and then a proton is transferred from this water to the second water (PT2) at 72 fs. Short afterwards, a proton of the second water moves to N2 in the pyridine ring (PT3) at 78 fs, and the tautomer (T) form is achieved within 79 fs. After completing the reaction, the complex dissociates.

Average values for geometric parameters and energies for the 9 trajectories following the ESTPT reaction are shown in Fig. 3 and 4, respectively. The evolution of the average values of three breaking bonds (N1—H1, O1—H2, and O2—H3) and three forming bonds (O1···H1, O2···H2 and N2···H3) is shown in Fig. 3(a). The intersection between the lines indicates that, on average, the first PT occurs at 50 fs when N1—H1 and O1—H1 bond lengths are equal to 1.299 Å, while the second PT occurs at 55 fs when O2—H3 and N2—H3 are equal to 1.339 Å, and the third PT occurs at 58 fs when O1—H2 and O2—H2 are equal to 1.270 Å (these values are compiled in Table 2). There is a certain time lag (∼5 fs) between first and second PT, and a 3 fs time lag between the second PT and the third PT. These results characterize the process as asynchronous concerted triple PT.

It is noteworthy to compare our dynamics results with those for 7AI$(H_2O)_2$ computed at state-specific CASSCF/DZP level reported by Kina et al. [40]. In that work, a single trajectory was computed with initial energy right above the threshold for PT. The ESTPT time was estimated to be 40–60 fs. The present result (58 fs) based on an average over an ensemble of trajectories is in close agreement with that of Ref. [40]. Fig. 4 shows that the average energy difference between $S_1(\pi\pi^*)$ and S_0 gradually decreases in the first 100 fs. After that, the average energy difference is above 40 kcal mol^{-1}, reflecting the structural planarity of the complex in the next 200 fs. This feature diverges from the dynamics results from Ref. [40]. There, the energy difference during the dynamics was about 20 kcal mol^{-1}, with ring-puckering oscillations bringing 7AI near a conical intersection. This result was interpreted as an indication that internal conversion could take place after the PT. Nevertheless, complementary calculations for the tautomer at the state averaged CASSCF and CASPT2 levels, also reported in Ref. [40], indicated rather larger energy differences (about 48 and

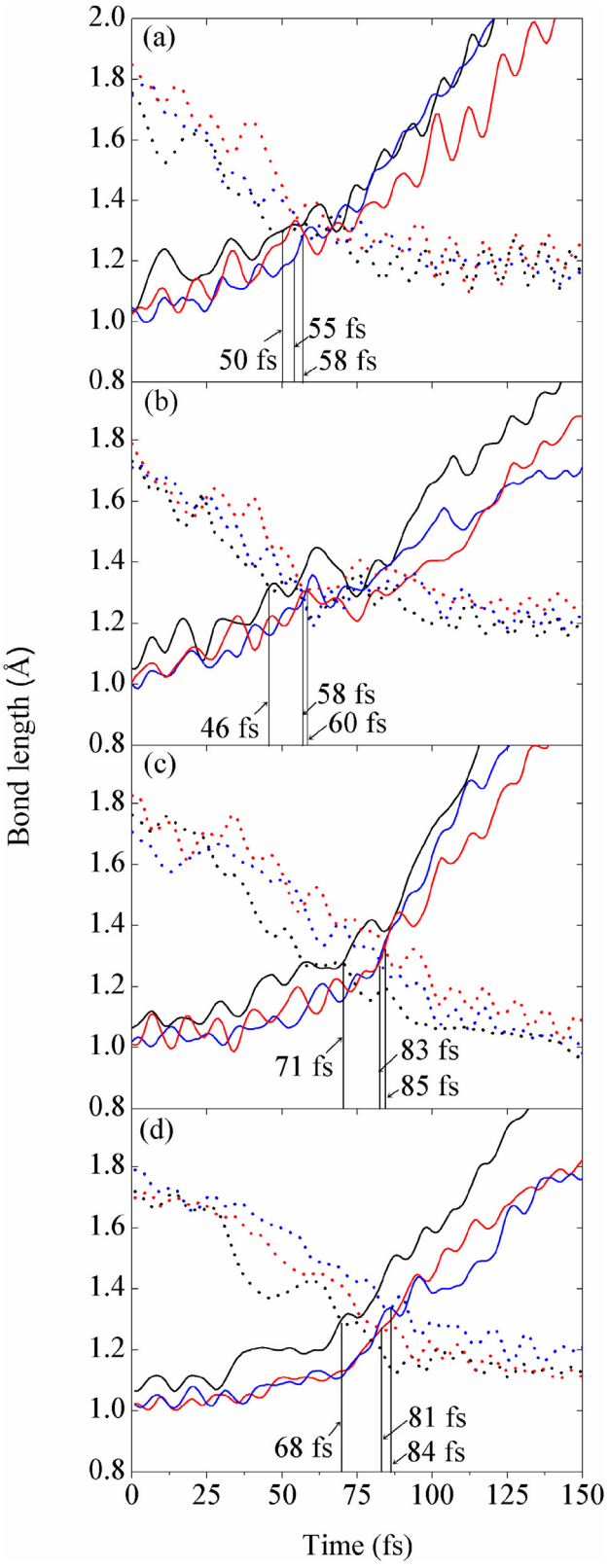

Fig. 3. Average breaking and forming bonds showing time evolution (PT time): (a) average value over 9 trajectories of the $7Al(H_2O)_2$ complex, (b) average values over 8 trajectories of the $7Al(H_2O–MeOH)$ complex, (c) average values over 11 trajectories of the $7Al(MeOH–H_2O)$ complex, and (d) average value over 16 trajectories of the $7Al(MeOH)_2$ complex. N1—H1 and O1···H1 in black, O1—H2 and O2···H2 in blue, and O2—H3 and N2···H3 in red. (For interpretation of the references to color in this figure legend, the reader is referred to the web version of this article.)

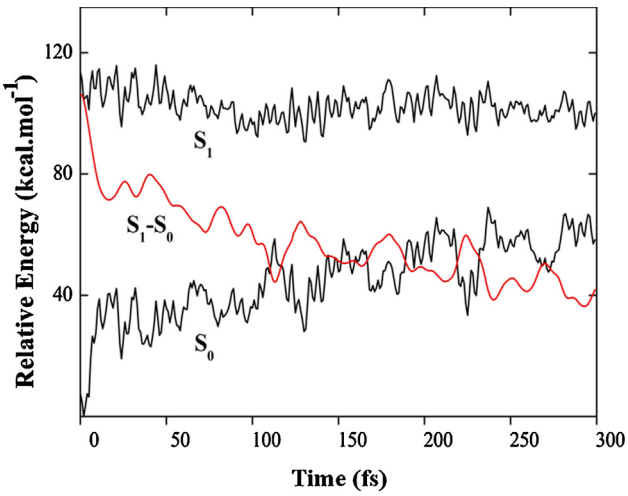

Fig. 4. Average potential energy diagram of complete reaction trajectories for $7Al(H_2O)_2$ complex in the ground state (S_0) and excited states ($\pi\pi^*$, $\pi\sigma^*$) performed at RI-ADC(2)/SVP-SV(P) level.

54 kcal mol^{-1}, respectively), which are closer to the present results. We cannot discard, however, the possibility of later internal conversion, because at the end of our simulations at 300 fs, the average energy difference was still not in the equilibrium regime (Fig. 4).

3.2.2. $7Al(H_2O–MeOH)$ complex

The ESTPT reaction occurred in 8 out of 25 trajectories, while no reaction was observed in 11 trajectories and 6 trajectories reached a region of degeneracy between $S_1(\pi\pi^*)$ and S_0. Therefore, the PT probability is 32%, slightly smaller than that for the $7Al(H_2O)_2$ complex (see Table 2). A representative trajectory (Fig. 5) illustrates how ESTPT reaction takes place. Starting from normal form (N), the process is summarized in the following three steps (the atom numbering is the same as defined in Fig. 1(b)): (1) a proton departs from N1 on pyrrole ring to O1 of the nearest water molecule (PT1) at 64 fs; (2) a proton moves from O1 of water to O2 of methanol (PT2) at 76 fs; and (3) a proton leaves O2 of methanol toward N2 on the pyridine ring (PT3) at 80 fs. For this trajectory, the complete ESPT reaction is obtained after 82 fs and followed by the complex dissociation.

The average values over 8 trajectories of the three breaking bonds (N1—H1, O1—H2, and O2—H3) increase, at the same time, the average values of the forming bonds (O1···H1, O2···H2 and N2···H3) decrease, as shown in Fig. 3(b). The first PT process occurs at 46 fs when the average N1—H1 and H1—O1 distances are equal to 1.328 Å (Table 2). The second proton transfers from water to methanol at 58 fs when the average O1—H2 and O2—H2 distances are equal to 1.290 Å. This leads to a certain time lag (~12 fs) between the first PT and second PT. The last PT occurs at 60 fs when the average O2—H3 and N2—H3 distances are equal to 1.311 Å. This dynamics behavior indicates an asynchronous concerted process.

3.2.3. $7Al(MeOH–H_2O)$ complex

For the $7Al(MeOH–H_2O)$ complex, 11 trajectories exhibited the ESTPT reaction, while 13 trajectories exhibited no reaction within the simulation time. Only one trajectory proceeded through $S_1(\pi\pi^*)/S_0$ crossing. Thus, the PT reaction probability is 44% (Table 2). A representative trajectory (Fig. 6) shows the ESTPT reaction as the proton moves along the hydrogen-bonded network. For this trajectory, the first, second, and third PT processes occur at 53, 69, and 81 fs, respectively, until the tautomer (T) is formed at 83 fs.

The atom numbering is the same as defined in Fig. 1(c). With the same criteria used in the $7Al(H_2O)_2$ and $7Al(H_2O–MeOH)$ complexes, we found that for $7Al(MeOH–H_2O)$ the average times are

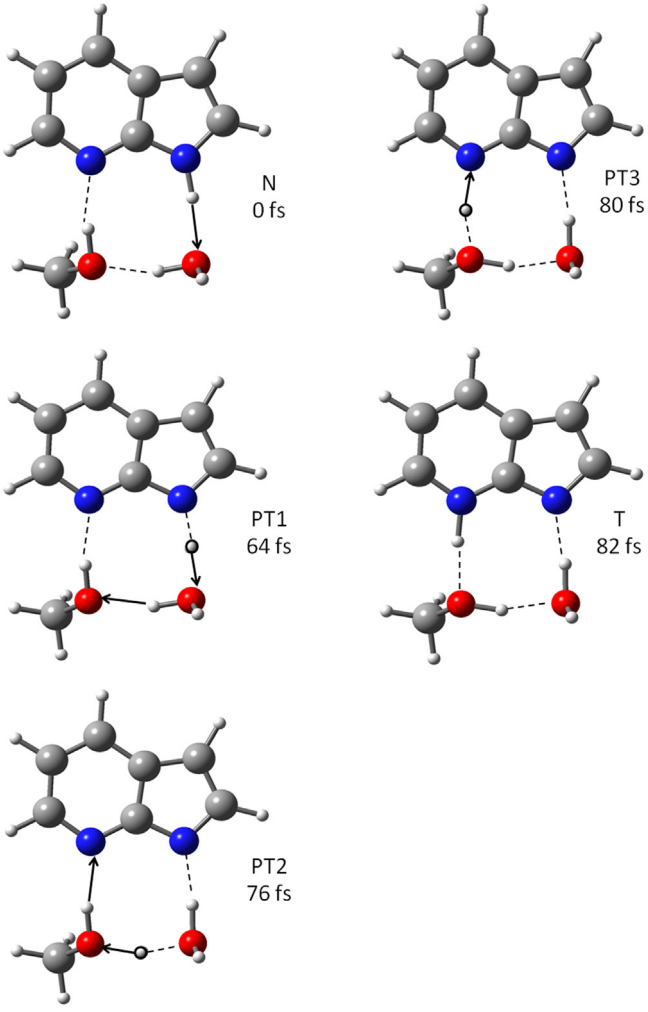

Fig. 5. Snapshots from a representative trajectory of the 7AI(H_2O–MeOH) complex, showing the time evolution of the ESTPT reaction through a hydrogen-bonded network within 82 fs. Averaged over all type-1 trajectories, this reaction is completed within 60 fs.

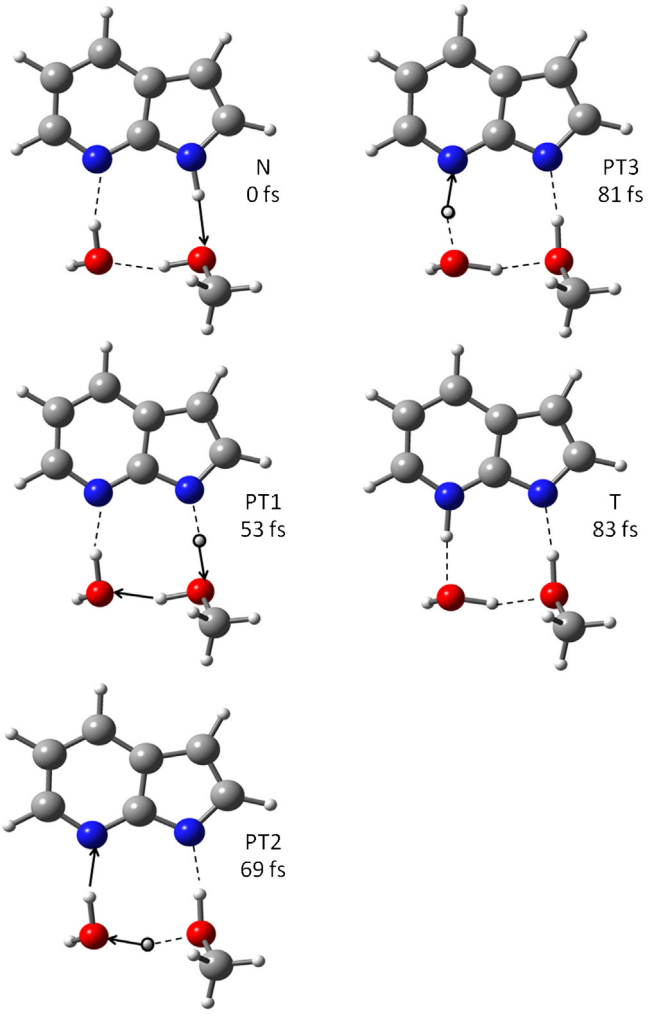

Fig. 6. Snapshots for a representative trajectory of the 7AI(MeOH–H_2O) complex showing the time evolution of the ESTPT reaction through a hydrogen-bonded network within 83 fs. Averaged over all type-1 trajectories, this reaction is completed within 85 fs.

71, 83, and 85 fs with bond distances of 1.279 Å (N1—H1=O1—H1), 1.295 Å (O1—H2=O2—H2), and 1.332 Å (O2—H3=N2—H3), respectively (see Fig. 3(c) and Table 2). There is a certain time lag (~12 fs) between the first PT and second PT, but time lags between the second PT and third PT is only 2 fs implying that the asynchronous concerted mechanism is also favorable for this complex.

3.2.4. 7AI(MeOH)$_2$ complex

In Ref. [20], we have reported dynamics results for 7AI(MeOH)$_n$ (n = 1–3) computed also at the RI-ADC(2)/SVP-SV(P) level used in this work. In this section, we summarize the data for 7AI(MeOH)$_2$ for a sake of completeness of the series of complexes investigated here. The ESTPT reactions occurred in 16 trajectories, while 5 trajectories showed no reaction within the simulation time and 4 trajectories reached a region of degeneracy of $S_1(\pi\pi^*)/S_0$. Therefore, the probability is 64%, which is the highest among all investigated complexes (Table 2).

Using the atom numbering defined in Fig. 1(d) and with the same criteria in other complexes, we found that for 7AI(MeOH)$_2$ the average times for the first, second and third PT are 68, 81, and 84 fs with bond distances 1.308 Å, 1.271 Å, and 1.334 Å, respectively (see Fig. 3(d) and Table 2). There is a certain time lag (~13 fs) between the first PT and second PT, but the time lag between the second PT and third PT is only 3 fs indicating that the asynchronous concerted mechanism is also favorable for this complex.

3.3. Time and barrier height for proton transfer

For all trajectories of type 1 (complete ESTPT) of each complex, we computed the average energies of the ground (S_0) and the first-excited ($\pi\pi^*$) states for the normal (N), intermediary (IS1, IS2, and IS3), and tautomer (T) structures along the reaction pathway. They are shown in Table 3 and Fig. 7.

The results in Table 3 and Fig. 7 show that the average excited-state reaction path has barriers of 3, 6, 2, and 2 kcal mol^{-1} for the 7AI(H_2O)$_2$, 7AI(H_2O–MeOH), 7AI(MeOH–H_2O), and 7AI(MeOH)$_2$, respectively. The average excited-state barriers nicely correlate with the PT probability reported in Table 2. In particular, it helps to rationalize why the probability of the PT reaction increases from 32% to 44% in the comparison between 7AI(H_2O–MeOH) and 7AI(MeOH–H_2O). Additionally, the larger excited-state barrier for 7AI(H_2O)$_2$ than for 7AI(MeOH)$_2$ is in good agreement with results reported by Fang et al. [22,23] using MRPT2/CASSCF method.

The excited-state barrier for tautomerization in 7AI is dramatically decreased when assisted with solvents (water or methanol) [22,23,41,54]. These solvent molecules play an important role in

Table 3
Average relative ground (S_0) and excited states ($\pi\pi^*$) energies (kcal mol^{-1}) of all type 1 trajectories for each complex for characteristic points.

State	Form	Complex			
		7AI(H_2O)$_2$	7AI(H_2O–MeOH)	7AI(MeOH–H_2O)	7AI(MeOH)$_2$
S_0	N	0	0	0	0
	IS1	36	37	32	36
	IS2	37	45	35	38
	IS3	35	46	37	40
	T	30	38	26	26
S_1 ($\pi\pi^*$)	N	104	104	101	103
	IS1	107	110	103	105
	IS2	103	106	99	104
	IS3	103	105	96	100
	T	98	101	88	89

reducing the activation energy of tautomerization and also in stabilizing 7AI tautomer. The role played by the solvent effect is more pronounced when replacing water with methanol [22,23] or partially replacing water with methanol, as in this current work. When increasing number of methanol or replacing it in place of water in the site near the pyrrole, the intermolecular hydrogen bonds between 7AI and methanol become stronger due to the attractive force interaction between them. This effect can certainly shift the excited-state barrier and also the probability of the PT reaction.

ESTPT in 7AI(H_2O–MeOH) and 7AI(H_2O)$_2$ is completed within 45–60 fs, whereas, ESTPT in 7AI(MeOH–H_2O) and 7AI(MeOH)$_2$ is completed within a slightly longer time, 70–85 fs. Our results show that methanol lowers the reaction barrier, increasing the PT probability. For the mixed water–methanol complexes, we have observed that if the water is positioned near the pyrrole moiety, dynamics results are similar to the results for the 7AI(H_2O)$_2$ complex. If, however, methanol is positioned near the pyrrole moiety, the results are similar to the results for 7AI(MeOH)$_2$. This implies that the first PT, from the pyrrole to the solvent molecule, is the rate determining step of the ESTPT reaction in these complexes.

Born–Oppenheimer dynamics simulations of light particles like protons may be subject to artifacts, especially because of the lack of quantum interference, neglecting of tunneling and missing nonadiabatic effects. As we discussed above, in the case of micro-solvated 7AI, the proton transfer occurs barrierless or with small barriers after the photoexcitation and there are no state crossing along the reaction pathway. When these two conditions are satisfied, all

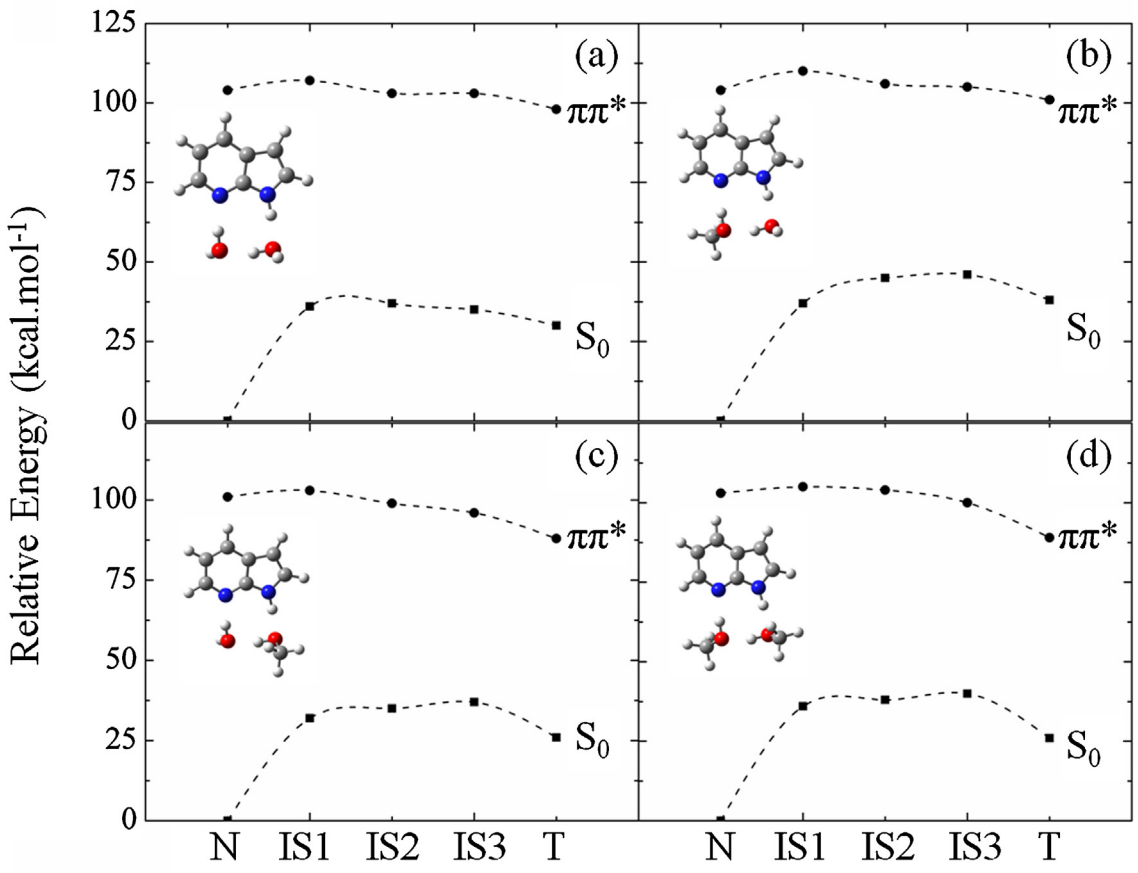

Fig. 7. Average relative energies (kcal mol^{-1}) of the ground (S_0) and the excited states ($\pi\pi^*$) of (a) 7AI(H_2O)$_2$, (b) 7AI(H_2O–MeOH), (c) 7AI(MeOH–H_2O), and (d) 7AI(MeOH)$_2$ complexes.

three quantum effects listed above are minimized and the proton transfer behaves as a ballistic process which can be treated classically. Moreover, our classical simulations have also been useful to detect the possibility of nonadiabatic effects occurring to a fraction of trajectories approaching the state crossing.

4. Conclusions

Excited-sate dynamics simulations were carried out for 7AI(H_2O)$_2$, 7AI(H_2O–MeOH), 7AI(MeOH–H_2O), and 7AI(MeOH)$_2$ complexes at RI-ADC(2)/SVP-SV(P) level. These simulations revealed that sub 100 fs excited-state proton transfer reactions may take place for all complexes.

The transfer process pathway is most likely a PT, suggested by no crossing between $\pi\pi^*$ and $\pi\sigma^*$ states for all complexes. The proton transfer probabilities are between 32 and 64% depending on the cluster. They are substantially larger when a MeOH is near the pyrrole ring than when a water molecule is there. Also PT times are slightly longer when MeOH is near the pyrrole ring. The average excited-state barriers of the first PT with clusters of 7AI having MeOH placed near pyrrole are lower than those clusters of 7AI having water near pyrrole. Thus, the PT from pyrrole position to the solvent molecule is most likely the rate determining step of the ESTPT reaction. This step plays an important role in characterization of the dynamics behavior such as time evolution and reaction probability. All ESTPT processes are completed within 85 fs and showed an asynchronous concerted mechanism, with a time lag lower than 15 fs regardless of the kind of solvent molecules.

Indication of internal conversion prior the proton transfer was observed in all clusters. No conclusive indication of internal conversion after the proton transfer was observed.

Acknowledgements

The authors wish to thank the Thailand Research Fund (MRG5480294 and RTA5380010) for financial support. They also would like to express grateful acknowledgment to the Department of Chemistry, Faculty of Science, Chiang Mai University. R. Daengngern and K. Kerdpol thank the Research Professional Development Project under the Science Achievement Scholarship of Thailand (SAST), Faculty of Science, Chiang Mai University, Chiang Mai, Thailand.

Appendix A. Supplementary data

Supplementary data associated with this article can be found, in the online version, at http://dx.doi.org/10.1016/j.jphotochem.2013.05.012.

References

[1] L.G. Arnaut, S.J. Formosinho, Excited-state proton transfer reactions. I. Fundamentals and intermolecular reactions, Journal of Photochemistry and Photobiology A 75 (1993) 1.
[2] S.J. Formosinho, L.G. Arnaut, Excited-state proton transfer reactions. II. Intramolecular reactions, Journal of Photochemistry and Photobiology A 75 (1993) 21.
[3] F.S. Rodembusch, F.P. Leusin, L.F. da Costa Medina, A. Brandelli, V. Stefani, Synthesis and spectroscopic characterisation of new ESIPT fluorescent protein probes, Photochemical & Photobiological Sciences 4 (2005) 254.
[4] T.-I. Kim, H.J. Kang, G. Han, S.J. Chung, Y. Kim, A highly selective fluorescent ESIPT probe for the dual specificity phosphatase MKP-6, Chemical Communications (Cambridge, UK) (2009) 5895.
[5] R. Morales Alma, J. Schafer-Hales Katherine, O. Yanez Ciceron, V. Bondar Mykhailo, V. Przhonska Olga, I. Marcus Adam, D. Belfield Kevin, Excited state intramolecular proton transfer and photophysics of a new fluorenyl two-photon fluorescent probe, Chemphyschem 10 (2009) 2073.
[6] P.T. Chou, S.L. Studer, M.L. Martinez, Practical and convenient 355-nm and 337-nm sharp-cut filters for multichannel Raman spectroscopy, Journal of Applied Spectroscopy 45 (1991) 513.
[7] S.M. Chang, Y.J. Tzeng, S.Y. Wu, K.Y. Li, K.L. Hsueh, Emission of white light from 2-(2′-hydroxyphenyl) benzothiazole in polymer electroluminescent devices, Thin Solid Films 477 (2005) 38.
[8] S.M. Chang, K.L. Hsueh, B.K. Huang, J.H. Wu, C.C. Liao, K.C. Lin, Solvent effect of excited state intramolecular proton transfer in 2-(2′-hydroxyphenyl) benzothiazole upon luminescent properties, Surface and Coatings Technology 200 (2006) 3278.
[9] J. Catalan, On the evidence obtained by exciting 7-azaindole at 320 nm in 10^{-2} M solutions. Reply, Journal of Physical Chemistry A 107 (2003) 5642.
[10] J. Catalan, On the molecular structure that produces the phosphorescence of 7-azaindole, International Journal of Quantum Chemistry 102 (2005) 489.
[11] J. Catalan, V.J.C. del, M. Kasha, Resolution of concerted versus sequential mechanisms in photo-induced double-proton transfer reaction in 7-azaindole H-bonded dimer, Proceedings of the National Academy of Sciences of the United States of America 96 (1999) 8338.
[12] J. Catalan, P. Perez, V.J.C. del, P.J.L.G. de, M. Kasha, H-bonded N-heterocyclic base-pair phototautomerizational potential barrier and mechanism: the 7-azaindole dimer, Proceedings of the National Academy of Sciences of the United States of America 101 (2004) 419.
[13] C.-P. Chang, H. Wen-Chi, K. Meng-Shin, P.-T. Chou, J.H. Clements, Acid catalysis of excited-state double-proton transfer in 7-azaindole, Journal of Physical Chemistry A 98 (1994) 8801.
[14] Y. Chen, F. Gai, J.W. Petrich, Solvation and excited-state proton transfer of 7-azaindole in alcohols, Chemical Physics Letters 222 (1994) 329.
[15] Y. Chen, R.L. Rich, F. Gai, J.W. Petrich, Fluorescent species of 7-azaindole and 7-azatryptophan in water, Journal of Physical Chemistry 97 (1993) 1770.
[16] P.T. Chou, M.L. Martinez, W.C. Cooper, S.T. Collins, D.P. McMorrow, M. Kasha, Monohydrate catalysis of excited-state double-proton transfer in 7-azaindole, Journal of Physical Chemistry 96 (1992) 5203.
[17] P.-T. Chou, C.-Y. Wei, C.-P. Chang, M.-S. Kuo, Structure and thermodynamics of 7-azaindole hydrogen-bonded complexes, Journal of Physical Chemistry 99 (1995) 11994.
[18] P.-T. Chou, C.-Y. Wei, G.-R. Wu, W.-S. Chen, Excited-state double proton transfer in 7-azaindole analogues: observation of molecular-based tuning proton-transfer tautomerism, Journal of the American Chemical Society 121 (1999) 12186.
[19] P.-T. Chou, W.-S. Yu, Y.-C. Chen, C.-Y. Wei, S.S. Martinez, Ground-state reverse double proton transfer of 7-azaindole, Journal of the American Chemical Society 120 (1998) 12927.
[20] R. Daengngern, N. Kungwan, P. Wolschann, A.J.A. Aquino, H. Lischka, M. Barbatti, Excited-state intermolecular proton transfer reactions of 7-azaindole(MeOH)$_n$ (n = 1–3) clusters in the gas phase: on-the-fly dynamics simulation, Journal of Physical Chemistry A 115 (2011) 14129.
[21] H. Fang, Y. Kim, Solvent effects in the excited-state tautomerization of 7-azaindole: a theoretical study, Journal of Physical Chemistry B 115 (2011) 15048.
[22] H. Fang, Y. Kim, Theoretical studies for excited-state tautomerization in the 7-azaindole-(CH_3OH)$_n$ (n = 1 and 2) complexes in the gas phase, Journal of Physical Chemistry A 115 (2011) 13743.
[23] H. Fang, Y. Kim, Excited-state tautomerization in the 7-azaindole-(H_2O)$_n$ (n = 1 and 2) complexes in the gas phase and in solution: a theoretical study, Journal of Chemical Theory and Computation 7 (2011) 642.
[24] D.E. Folmer, E.S. Wisniewski, S.M. Hurley, A.W. Castleman Jr., Femtosecond cluster studies of the solvated 7-azaindole excited state double-proton transfer, Proceedings of the National Academy of Sciences of the United States of America 96 (1999) 12980.
[25] D.E. Folmer, E.S. Wisniewski, J.R. Stairs, A.W. Castleman, Water-assisted proton transfer in the monomer of 7-azaindole†, Journal of Physical Chemistry A 104 (2000) 10545.
[26] W.-T. Hsieh, C.-C. Hsieh, C.-H. Lai, Y.-M. Cheng, M.-L. Ho, K.K. Wang, G.-H. Lee, P.-T. Chou, Excited-state double proton transfer in model base pairs: the stepwise reaction on the heterodimer of 7-azaindole analogues, Chemphyschem 9 (2008) 293.
[27] Y. Kageura, K. Sakota, H. Sekiya, Charge transfer interaction of intermolecular hydrogen bonds in 7-azaindole(MeOH)$_n$ (n = 1, 2) with IR-Dip spectroscopy and natural bond orbital analysis, Journal of Physical Chemistry A 113 (2009) 6880.
[28] O.-H. Kwon, A.H. Zewail, Double proton transfer dynamics of model DNA base pairs in the condensed phase, Proceedings of the National Academy of Sciences of the United States of America 104 (2007) 8703.
[29] K. Sakota, N. Inoue, Y. Komoto, H. Sekiya, Cooperative triple-proton/hydrogen atom relay in 7-azaindole(CH_3OH)$_2$ in the gas phase: remarkable change in the reaction mechanism from vibrational-mode specific to statistical fashion with increasing internal energy, Journal of Physical Chemistry A 111 (2007) 4596.
[30] K. Sakota, C. Jouvet, C. Dedonder, M. Fujii, H. Sekiya, Excited state triple-proton transfer in 7-azaindole(H_2O)$_2$ and reaction path studied, Journal of Physical Chemistry A 114 (2010) 11161.
[31] K. Sakota, Y. Kageura, H. Sekiya, Cooperativity of hydrogen-bonded networks in 7-azaindole(CH_3OH)$_n$ (n = 2, 3) clusters evidenced by IR-UV ion-dip spectroscopy and natural bond orbital analysis, Journal of Chemical Physics 129 (2008), 054303/1.
[32] K. Sakota, Y. Komoto, M. Nakagaki, W. Ishikawa, H. Sekiya, Observation of a catalytic proton/hydrogen atom relay in microsolvated 7-azaindole-methanol cluster enhanced by a cooperative motion of the hydrogen-bonded network, Chemical Physics Letters 435 (2007) 1.

[33] K. Sakota, N. Komure, W. Ishikawa, H. Sekiya, Spectroscopic study on the structural isomers of 7-azaindole(ethanol)$_n$ (n = 1–3) and multiple-proton transfer reactions in the gas phase, Journal of Chemical Physics 130 (2009), 224307/1.
[34] A.S. Smirnov, D.S. English, R.L. Rich, J. Lane, L. Teyton, A.W. Schwabacher, S. Luo, R.W. Thornburg, J.W. Petrich, Photophysics and biological applications of 7-azaindole and its analogs, Journal of Physical Chemistry B 101 (1997) 2758.
[35] C.A. Taylor, M.A. El-Bayoumi, M. Kasha, Excited-state two-proton tautomerism in hydrogen-bonded N-heterocyclic base pairs, Proceedings of the National Academy of Sciences of the United States of America 63 (1969) 253.
[36] S.-B. Zhao, S. Wang, Luminescence and reactivity of 7-azaindole derivatives and complexes, Chemical Society Reviews 39 (2010) 3142.
[37] A.H. Zewail, Femtochemistry. Past, present, and future, Pure and Applied Chemistry 72 (2000) 2219.
[38] M.P.T. Duong, Y. Kim, Theoretical studies for the rates and kinetic isotope effects of the excited-state double proton transfer in the 1:1 7-azaindole:H_2O complex using variational transition state theory including multidimensional tunneling, Journal of Physical Chemistry A 114 (2010) 3403.
[39] M.P.T. Duong, K. Park, Y. Kim, Excited state double proton transfer of a 1:1 7-azaindole:H_2O complex and the breakdown of the rule of the geometric mean: variational transition state theory studies including multidimensional tunneling, Journal of Photochemistry and Photobiology A 214 (2010) 100.
[40] D. Kina, A. Nakayama, T. Noro, T. Taketsugu, M.S. Gordon, Ab initio QM/MM molecular dynamics study on the excited-state hydrogen transfer of 7-azaindole in water solution, Journal of Physical Chemistry A 112 (2008) 9675.
[41] G.M. Chaban, M.S. Gordon, The ground and excited state hydrogen transfer potential energy surface in 7-azaindole, Journal of Physical Chemistry A 103 (1999) 185.
[42] R.S. Moog, M. Maroncelli, 7-Azaindole in alcohols: solvation dynamics and proton transfer, Journal of Physical Chemistry 95 (1991) 10359.
[43] M.N.R. Ashfold, B. Cronin, A.L. Devine, R.N. Dixon, M.G.D. Nix, The role of $\pi\sigma^*$ excited states in the photodissociation of heteroaromatic molecules, Science (Washington, DC, United States) 312 (2006) 1637.
[44] C. Tanner, C. Manca, S. Leutwyler, Probing the threshold to H atom transfer along a hydrogen-bonded ammonia wire, Science (Washington, DC, United States) 302 (2003) 1736.
[45] C. Tanner, C. Manca, S. Leutwyler, Exploring excited-state hydrogen atom transfer along an ammonia wire cluster: competitive reaction paths and vibrational mode selectivity, Journal of Chemical Physics 122 (2005), 204326/1.
[46] C. Tanner, M. Thut, A. Steinlin, C. Manca, S. Leutwyler, Excited-state hydrogen-atom transfer along solvent wires: water molecules stop the transfer, Journal of Physical Chemistry A 110 (2006) 1758.
[47] C. Hättig, Geometry optimizations with the coupled-cluster model CC2 using the resolution-of-the-identity approximation, Journal of Chemical Physics 118 (2003) 7751.
[48] C. Hättig, Structure optimizations for excited states with correlated second-order methods: CC2 and ADC(2), Advances in Quantum Chemistry 50 (2005) 37.
[49] R. Ahlrichs, M. Bär, M. Häser, H. Horn, C. Kölmel, Electronic structure calculations on workstation computers: the program system TURBOMOLE, Chemical Physics Letters 162 (1989) 165.
[50] R. Ahlrichs, M. Bär, M. Häser, C. Kölmel, J. Sauer, Nonempirical direct SCF calculations on sodalite and double six-ring models of silica and aluminum phosphate (AlPO4) minerals: $H_{24}Si_{24}O_{60}$, $H_{12}Si_{12}O_{30}$, $H_{12}A_{l6}P_6O_{30}$, Chemical Physics Letters 164 (1989) 199.
[51] A. Schäfer, H. Horn, R. Ahlrichs, Fully optimized contracted Gaussian basis sets for atoms lithium to krypton, Journal of Chemical Physics 97 (1992) 2571.
[52] M. Barbatti, G. Granucci, M. Persico, M. Ruckenbauer, M. Vazdar, M. Eckert-Maksić, H. Lischka, The on-the-fly surface-hopping program system Newton-X: application to ab initio simulation of the nonadiabatic photodynamics of benchmark systems, Journal of Photochemistry and Photobiology A 190 (2007) 228.
[53] M. Barbatti, G. Granucci, M. Ruckenbauer, F. Plasser, J. Pittner, M. Persico, H. Lischka, Newton-X: a package for Newtonian dynamics close to the crossing seam, version 1.1, 2011 www.newtonx.org
[54] M.S. Gordon, Hydrogen transfer in 7-azaindole, Journal of Physical Chemistry 100 (1996) 3974.